INTERNATIONAL JOURNAL OF AUTOMOTIVE AND MECHANICAL ENGINEERING (IJAME)
ISSN: 2229-8649 e-ISSN: 2180-1606
VOL. 18, ISSUE 1, 8464 – 8477
DOI: https://doi.org/10.15282/ijame.18.1.2021.06.0641

ORIGINAL ARTICLE

Prognostics of Induction Motor Shaft Based on Feature Importance and Least Square Support Vector Machine Regression

D.D. Susilo[1*], A. Widodo[2], T. Prahasto[2] and M. Nizam[3]

[1]Department of Mechanical Engineering, Faculty of Engineering, Universitas Sebelas Maret, Ir. Sutami Street, 36A, Surakarta, Indonesia
Phone: +62271632163; Fax: +62271632163
[2]Department of Mechanical Engineering, Faculty of Engineering, Universitas Diponegoro, Prof Sudarto Street, Semarang, Indonesia
[3]Department of Electrical Engineering, Faculty of Engineering, Universitas Sebelas Maret, Ir. Sutami Street, 36A, Surakarta, Indonesia

ABSTRACT – This paper aims to present a prognostic method for induction motor shafts that experience fatigue failure in the keyway area, using motor vibration signals. Preprocessing the data to eliminate noise in raw signals is done by decomposing the signal, using discrete wavelet transforms. Prognostic indicator candidates are obtained through the selection of features based on its importance, which involve the superposition of monotonicity and trendability parameters. The prognostics model is built based on the least squares support vector machine regression approach. Remaining useful life (RUL) estimates of motor shafts were performed by fitting the sum of two exponential functions to the regression results and extrapolating over time until the specified failure threshold hits. The results of the study show that the proposed method can work satisfactorily to estimate the RUL of motor shaft. The best prognostic indicator namely the RMS, can be used to predict the motor shaft RUL since 50% of the time step before the end of the motor shaft life is error bound within 20%.

ARTICLE HISTORY
Received: 29th Jan 2020
Revised: 28th Oct 2020
Accepted: 7th Jan 2021

KEYWORDS
Induction motor shaft; feature importance; LSSVM regression; RUL estimation

INTRODUCTION

Induction motors are electromechanical devices that convert energy from electrical to mechanical form. They are widely used as prime movers in modern industrial applications. The induction motors are combined with mechanical devices such as pumps, fans, compressors, mechanical transmission drives, machine tools, and conveyor belts to accomplish the safe and efficient operation of industrial plants. This is due to their superiority in terms of robustness, simplicity of construction, reliability, low cost, and wide range of power [1]. The induction motor is connected to the mechanical devices using coupling or a pulley through the shaft. The most common material of the shaft is a hot rolled carbon steel. Alloyed steel, such as chromium-molybdenum, is frequently used for higher load applications and a stainless-steel shaft for corrosive environments.

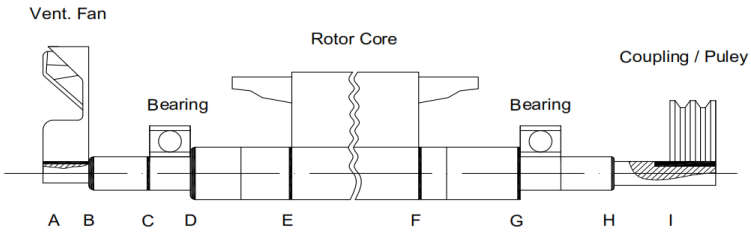

Figure 1. Typical motor shaft assembly cross-section.

Figure 1 illustrates a typical motor shaft assembly. It shows that the shaft geometry is always stepped as a rotor core with a maximum diameter in the middle and a minimum diameter at the ends to provide shoulders for positioning the coupling or pulley and ventilating fan. The bearings are mounted to support the shaft. The fillet radius prevents stress concentration due to an abrupt change in the cross-section. Commonly, the motor load is imposed at the coupling or pulley join. As the motor operates, the shaft receives a fluctuating load of combined bending and torsion with various degrees of stress concentration. For such a shaft, the problem is fatigue loading that can cause motor shaft fatigue failure [2]. The points F, G, H, and I in Figure 1 are the most vulnerable areas because of surface discontinuity. Mostly, shafts fail due to cracks initiated along the keyway region (Area I), as a result of high-stress concentrations caused due to sharp edges having less stress relief radii [2–6].

*CORRESPONDING AUTHOR | D. D. Susilo | djoksus@uns.ac.id

The failure of the motor shaft can break the plant operation that leads to the loss of production, even sometimes brings about safety issues. Therefore, the maintenance of an induction motor is essential to ensure its performance becomes critical in a plant maintenance policy. Condition-based maintenance (CBM) is a maintenance philosophy that actively manages the health condition of the assets. The maintenance action depends on the assets requirement. This strategy usually uses machine run-time data to monitor the asset's condition. Diagnostics and prognostics are two essential aspects of the CBM program. Diagnostics refers to detecting, isolating, and identifying an incipient failure condition, while prognostics deals with fault prediction include the remaining useful life (RUL) estimation [7]. Research in the field of induction motor diagnostics has developed rapidly in the two last decades. Various methods for diagnosing the induction motor faults, including electrical and mechanical faults, have been investigated. Traditional methods such as vibration monitoring, motor current signature analysis, torque monitoring, temperature monitoring, and advanced diagnostic techniques using artificial intelligence (AI) such as artificial neural networks, neuro-fuzzy logic, and support vector machines have been proposed by researchers to detect the induction motor faults, as reviewed by [8–14].

Meanwhile, the publication in the field of induction motor prognostics is limited compared to the field of diagnostics. Indeed, the task of prognosis in predicting the development of component degradation trends and estimating the RUL is not easy. However, researchers have worked hard to develop methods of prognostics of the induction motors and mechanical drive systems, some of which are presented here. Kraleti et al. [15] developed a model-based fault detection approach for a three-phase induction motor experiencing insulation degradation and a broken rotor. They employed a neural network to discover the system parameter degradation to predict motor failure. Arora et al. [16] proposed a fuzzy logic-based first order log-log electro-thermal life model to estimate the life of an induction motor under non-sinusoidal voltage and current waveforms. The motor insulation was subjected to multiple stresses and resulted in accelerated ageing, which led to the induction motor's failure. Subsequently, the model was used to estimate the percentage of the life of the induction motor. Gaeid [17] presented the wavelet index to detect the stator winding fault of the induction motor. Then, he used the index as a prognosis parameter to determine the severity of the fault. However, he had not calculated the remaining useful life of the induction motor after an experienced stator winding fault. Babel and Strangas [18] introduced a prognostics method for assessing the condition of a stator winding insulation of the electric machine and predicting its failure. The degradation of the insulation was simulated by altering the permittivity and conductivity of the insulation in a finite element model. They predicted RUL by fitting an exponential decay model on the insulation current measurement.

Barbieri et al. [19] presented a prognostics procedure that was applied to a three-phase induction motor. The procedure involved the generation of prognostics parameters using the genetic algorithm (GA) and ordinary least squares (OLS) method. They used the general path model to predict RUL. They found that the OLS method, on average, generated the best prognostics parameter performance, using a combination of time-domain features. Singleton et al. [20] introduced a data-driven methodology to predict the RUL of a bearing from vibration data. An exponential function was used to approximate the degradation data obtained from the feature extraction process. The extended Kalman filter was used to optimise the model parameter and predict the RUL of the bearing. Nguyen et.al. [21] proposed an exponential decay model to approach the degradation function of induction machine under an inter-turn fault. The model introduced the insulation resistance of the stator winding fault as the prognostic parameter. Then, the model parameter for the RUL estimation was obtained using a particle filter (PF) algorithm. Ahmad et al. [22] presented element bearing prognostics, utilising a regression-based adaptive predictive model. They used vibration RMS as the prognostic parameter and found that the proposed method was effective in determining the time to start prediction (TSP). Moreover, the model excellently estimated the bearing RUL. Jain and Lad [23] developed the innovative design of a generic Tool Condition Monitoring system that accounts for real-life future degradation profile viz. low, medium, and severe profile. They modelled the physics of evolution of a dynamic operating profile that evolves in a deterministic and uncertain way. The model developed was applied to estimate the RUL of cutting tool using vibration signal. The results showed that the proposed model outperforms the traditional approach. Yang et al. [24] proposed a nonlinear degradation Health Index (HI) to predict the remaining useful life of the induction motor. They found that exponential convex HI was more suitable to model the degradation of the induction motor. They also compared the neural network and the linear support vector regression model in predicting RUL. They showed that the neural network performance is better than the linear support vector regression.

Most of the publications above focus on the prognostics of failure in induction motor components such as rotor, motor insulation, stator winding failure and rotor bearing. The researchers have not paid attention to the prognostics of the induction motor shaft. Even though, in practice, the motor shaft plays an important role. It transmits power or torque to other mechanical devices. Consequently, the motor shaft continuously receives various loadings, such as bending stress, shear stress, and fatigue stress. Even the shaft receives axial torque load when operating at high speed [25]. All of these loads can lead to shaft failure. The common mechanisms of shaft failure are fatigue failure, overload failure, corrosion, and wear; with fatigue failure being the most frequently observed [26]. This paper examines an induction motor whose shaft is damaged due to continuous bending load.

This paper aims to present a new method for induction motor shafts prognostics using vibration data of the motor. The crucial step in the prognostic is the prognostic parameter determination. This paper proposes the parameter selection based on the Feature Importance (FI) value. This value is calculated from the feature monotonicity and trendability characteristic. The FI value is evaluated for the different number of training data. Feature with the highest FI and good trendability is the best candidate for prognostic parameter. The prognostic model is generated using a machine learning technique, namely the least square support vector machine (LS-SVM).

METHODOLOGY

Data Collection

The data used in testing the proposed prognostic model is laboratory data obtained from run-to-failure testing. The induction motor was operated until failure. A bending load of 1.5 times the normal capacity of the motor was imposed through a hydraulic power pack system to accelerate the failure. The run-to-failure test rig is shown in Figure 2. The induction motor was at a speed of 1450 rpm by setting the inverter to 50 Hz. The vibration signals were measured using two PCB 352C33 accelerometers attached to the motor casing by a magnetic base. They were sampled at a sampling frequency of 20 kHz and recorded every 10 minutes for 1 second.

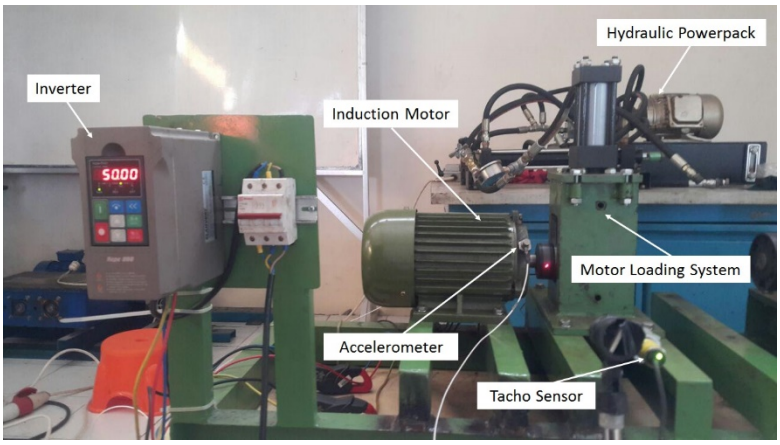

Figure 2. Motor run-to-failure test rig.

Data denoising

Raw vibration signals from the motor measurements are generally redundant and noisy, therefore, important information about the condition of the motor is hidden. Thus, data pre-processing is required to eliminate noisy signals. This was done using a discrete wavelet transform (DWT). The DWT is derived from the discretization of the continuous wavelet transform (CWT). It is given by [27] as follows:

$$DWT(j,k) = \int_{-\infty}^{+\infty} f(t) 2^{j/2} \psi^{*}(2^{j}t - k)dt \tag{1}$$

where, $DWT(j,k)$ are the wavelet transform coefficients, j is the level that is related to the frequency domain of the signal, k is in relation to the time domain. $f(t)$ is the signal and ψ is the wavelet used.

In the wavelet analysis, the signal is broken into approximation and detail coefficients. The approximation corresponds to low-frequency components, while the detail corresponds to high-frequency components. The approximation was then broken into a second-level approximation and detail, and the process was repeated to obtain the optimal result. This is formulated as in Eq. (2).

$$f(t) = \sum_{i=1}^{i=j} D_i(t) + A_j(t) \tag{2}$$

where, $D_i(t)$ denotes the wavelet detail, and $A_j(t)$ represents the approximation at the j level. The maximum number of decomposition levels depend on the number of data points. The principle of multi-resolution is demonstrated in Figure 3 for a four-level decomposition.

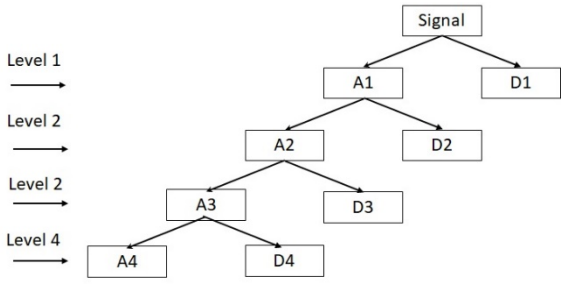

Figure 3. Discrete wavelet transform decomposition tree for four-level decomposition.

Feature extraction and selection

The raw data from the measurement of the vibration signals must be converted into the quantity that can provide information about the condition of the motor shaft, especially its degradation. It is done through feature extraction. Features that represent the motor health conditions can be the time domain features, the frequency domain features and the auto-regression estimation features. The features evaluated in this paper are presented in Table 1.

Table 1. Features extracted from the raw vibration signals.

No	Feature
1	Mean
2	Root mean square
3	Shape factor
4	Skewness
5	Kurtosis
6	Crest factor
7	Entropy estimation
8	Entropy estimation error
9	Histogram upper bound
10	Histogram lower bound
11	Root mean square frequency
12	Frequency centre
13	Root variance frequency
14	2nd auto-regression coefficient
15	3rd auto-regression coefficient
16	4th auto-regression coefficient
17	5th auto-regression coefficient

However, not all features are sensitive to the changes in motor conditions, while the prognostic process requires an indicator sensitive to changes in motor condition. Therefore, we need a method for selecting features to be used as an indicator of the prognostic. In this paper, we used the term feature importance (FI) to nominate them as an indicator of the prognostic. The FI is constructed from the superposition of the monotonicity and trendability of the features. The monotonicity characterises the underlying positive or negative trend of the parameter. Meanwhile, the trendability indicates the degree to which the parameters of a population of systems have the same underlying shape and can be described by the same functional form. Those criteria are formulated in [28] as follows:

$$Monotonicity = \left| \frac{Num.of\ d/dx > 0}{n-1} - \frac{Num.of\ d/dx < 0}{n-1} \right| \tag{3}$$

$$R = \frac{n(\sum xy) - (\sum x)(\sum y)}{\sqrt{\left[n\sum x^2 - (\sum x)^2\right]\left[n\sum y^2 - (\sum y)^2\right]}} \tag{4}$$

where R is the correlation coefficient between feature x and time index y. The features selection is based on the FI value of each feature. The feature with the highest FI was used as the prognostic indicator.

Degradation Model Development

The prediction model is built in two steps. The first step is to estimate the function of the training data through the LS-SVM regression. The training data comes from the results of the feature selection. The amount of training data is updated with the new measurement data. The second step is the process of fitting the motor shaft degradation curve, which was estimated using the LS-SVM regression with the sum of two exponential functions. Furthermore, the prediction model obtained was extrapolated to the specified failure threshold to estimate the RUL of the induction motor shaft.

Least squares support vector machine (LS-SVM)

The LS-SVM is derived from the prominent machine learning technique, namely a support vector machine (SVM). The algorithm of the SVM is to obtain an optimal separating hyperplane that separates different classes of data. The LS-SVM is a reformulation of the standard SVMs, which have been brought to solve the linear Karush Kuhn Tucker (KKT) system. The LS-SVM is closely related to the regularisation network and Gaussian processes but additionally emphasise and exploit the primal-dual interpretation. The LS-SVM formulation assigns the quality constraints and sum-squared error (SSE) cost functions, instead of the quadratic program in traditional SVMs. The theory of the LS-SVM is described by [28].

Assume first, a model in the primal weight space in the following form:

$$y(x) = w^T \varphi(x) + b \tag{5}$$

where $x \in \Re^n, y \in \Re, \varphi(.) : \Re^n \to \Re^{nh}$ is the mapping into the high dimensional space and potential infinite feature space. Providing a training set $\{x_k, y_k\}_{k=1}^N$, we can formulate the following optimisation problem in the primal weight space:

$$\min J_p(w, \varepsilon) = \frac{1}{2} w^T w + \gamma \frac{1}{2} \sum_{k=1}^{N} \varepsilon_k^2$$

Such that,

$$y_i = w^T \varphi(x_i) + b + \varepsilon_i, \quad i = 1, ..., N \tag{6}$$

where the fitting error is ε_i denoted by . The γ hyper- parameter controls the trade-off between the smoothness of the function and the accuracy of the fitting. This optimisation problem leads to the following solution below:

$$\hat{f}(x) = \sum_{i=1}^{N} \alpha_i K(x, x_i) + b \tag{7}$$

where, α_i are the coefficients and $K(x, x_i) = \varphi(x)\varphi(x_i)$ is the kernel. A common choice for the kernel is the Gaussian RBF:

$$K(x, x_i) = \exp - \frac{\|x - x_i\|^2}{2\sigma^2} \tag{8}$$

The main benefit of the LS-SVM technique is that it transforms the traditional quadratic problem into a simultaneous linear system problem, thus ensuring simplicity in computations and fast convergence. The LSSVM regression produce data pairs {Yp*, x*}, where Yp* is the matrix of prediction values of the training data, and x* is the matrix of the sample time. This data pair represents the degradation of the motor shaft.

Sum of two exponential functions

The exponential degradation model has been used by researchers to model the deterioration in the condition of a mechanical component. Some researchers use a single exponential model such as [29–31], while other researchers use a double exponential model [32,33]. This paper uses the sum of two exponential functions to fit the degradation evolution of the motor shaft presented by the data pairs {Yp*,x*}. The function is derived as follows:

$$Yp^*(x^*) = ae^{bx^*} + ce^{dx^*} \tag{9}$$

where, Yp* is the motor shaft condition, x* is the sample time and a, b, c and d are the fitted coefficients obtained from the non-linear least-squares method.

RUL Estimation and Performance Evaluation

The RUL of the motor shaft is estimated from the degradation evolution curve. The fitted model is extrapolated along the sample time until the model crossed the failure threshold. The threshold takes the maximum value of the prognostic indicator as illustrated in Figure 4.

The RUL of the motor shaft is calculated using the formula as follows:

$$RUL_{actual} = t_{EOL} - t_p \tag{10}$$

$$RUL_{prediction} = t_{EOP} - t_p \tag{11}$$

where t_{EOL} is the time index of the actual end of life, t_{EOP} is the earliest time index when the prediction has crossed the failure threshold and t_p is the time index at which the first prediction was made. The performance of the motor shaft RUL estimation using the proposed method was measured using the RUL error and root mean square error (RMSE). These parameters are formulated as follows:

$$RUL_{error} = RUL_{actual} - RUL_{predicted} \tag{12}$$

$$RMSE = \sqrt{\frac{1}{N}\sum_{i=1}^{n}\left|y_i^* - y_i^p\right|^2} \tag{13}$$

where, N is the number of the prediction, y_i* is the measured data at time *i* and y^p_i is the predicted value at time *i*.

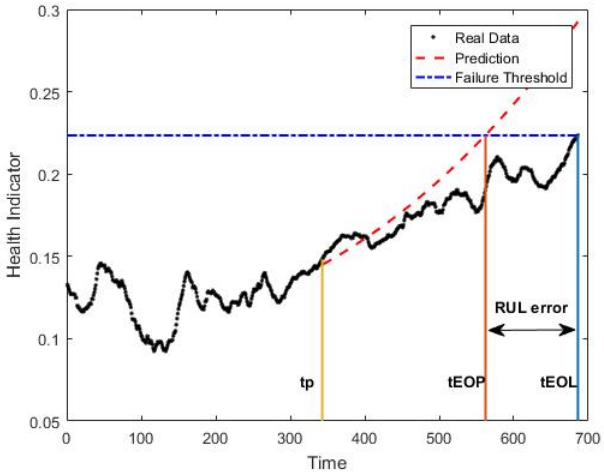

Figure 4. RUL prediction.

Furthermore, to compare the prediction performance of the RUL motor shaft estimation using different features, we used the α – λ accuracy plot. This plot is defined as a binary metric that evaluates whether the prediction accuracy at a specific time instance t_λ, falls within specified α-bounds. Here, t_λ is a fraction of time between t_P and the actual t_{EOL}. The α-bounds here are expressed as a percentage of the actual RUL r(i_λ) at t_λ. It is formulated in [34] as follows:

$$\alpha - \lambda\, accuracy = \begin{cases} 1 & if\ \ (1-\alpha).r_*(i) \le r^l(i) \le (1+\alpha).r_*(i) \\ 0 & otherwise \end{cases} \tag{14}$$

where, α is the accuracy modifier and λ is time window modifier, such that $t_\lambda = t_p + \lambda(t_{EOL} - t_p)$. In this paper, α is taken as 0.2 and λ is taken as 0.5.

RESULTS AND DISCUSSION

The induction motor runs continuously until reaching the failure threshold. The threshold was predetermined based on the magnitude of the vibration levels. The motor was stopped after the vibration amplitude was more than twice the initial amplitude and was taken as the failure threshold. A physical inspection of the motor shaft showed it to be a keyway failure, as illustrated in Figure 5. The raw vibration signal resulted from the run-to-failure testing is shown in Figure 6. It can be seen that it is mixed with noise. Therefore, a discrete wavelet transform (DWT) is performed to eliminate the noise. The decomposition is done until the 4th level. Figure 7 shows the result of signal decomposition.

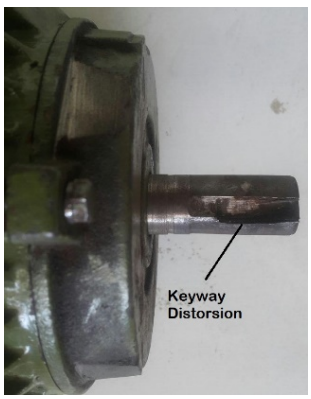

Figure 5. The keyway failure on the motor shaft.

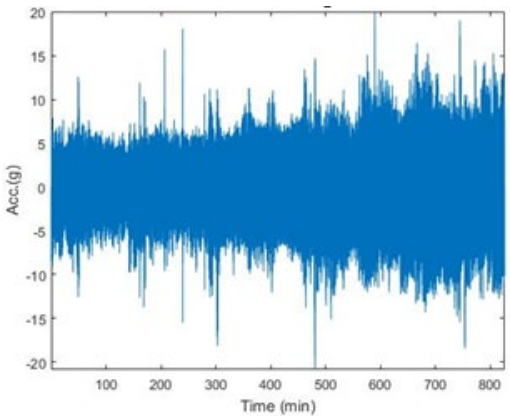

Figure 6. Raw vibration signal of the induction motor with shaft failure.

Figure 7 shows clearly that the vibration amplitude experiences a significant increase after 300 minutes, an indication of the initial damage. The features are extracted to trace the damage propagation. Seventeen features are obtained from 826 samples of vibration signals. Next, the features are smoothed using a moving average filter. An example of the smoothed RMS feature is presented in Figure 8. It shows the value of the RMS feature reaching a maximum at the sample number of 688. So, it assumes that the shaft fails at this point. This sample number is treated as the total run-to-failure data.

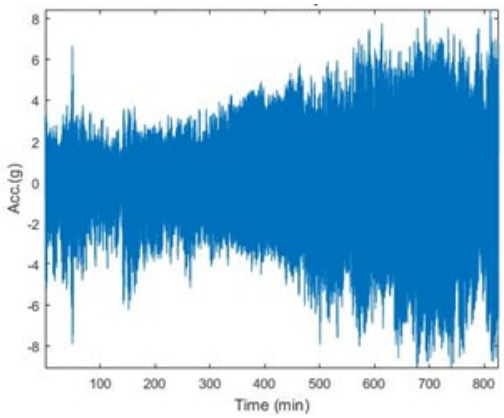

Figure 7. 4th level decomposition of the raw signal using DWT.

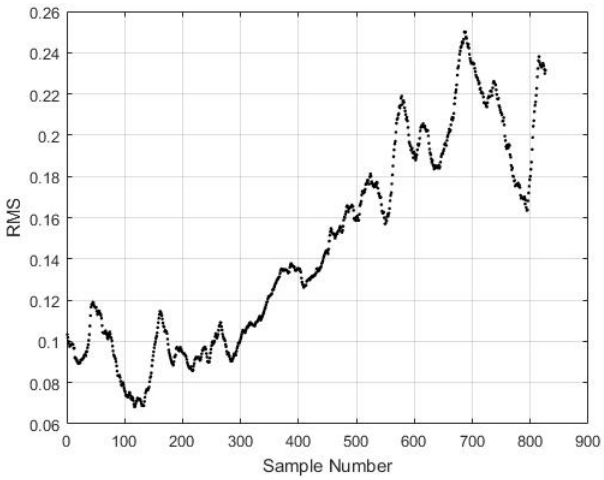

Figure 8. An example of the feature after smoothing.

However, not all of the features able to figure the damage propagation. The FI value is used as a criterion for feature selection. The FI values of the features are calculated at a different number of training data. They are taken as the percentage to the total of the training data as shown in Figure 9. It is evident from Figure 9 that three features have a high FI value, namely the RMS, entropy estimation, and histogram upper bound. Therefore, they become candidates of the prognostic indicator for estimating the motor shaft RUL. Additionally, the FI value of these three features tends to increase with the increasing amount of training data. This increase occurred after the amount of training data grew by 50%. The time related to this data is chosen as the prediction start time, t_P. This time was updated for each additional training data

of 10%, until the end of the life cycle of the motor shaft life. The three selected features are shown in Figure 10(a) to 10(c).

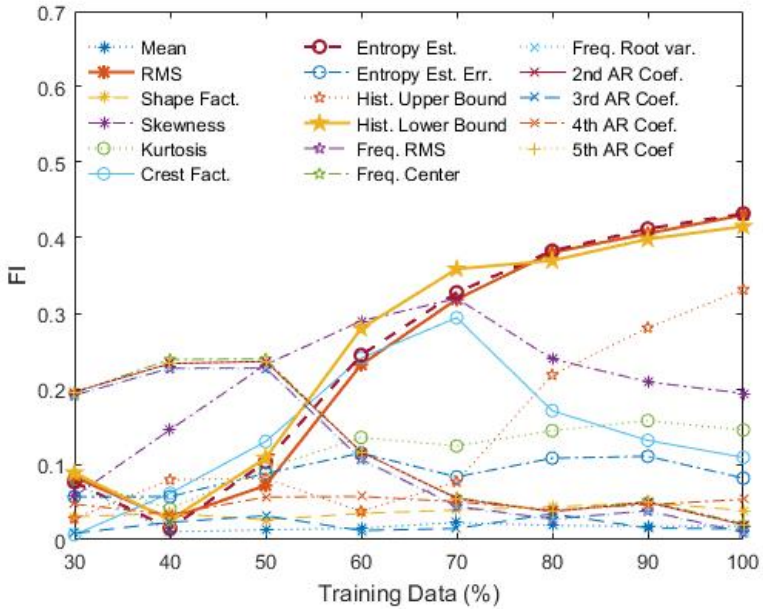

Figure 9. The feature importance of the features

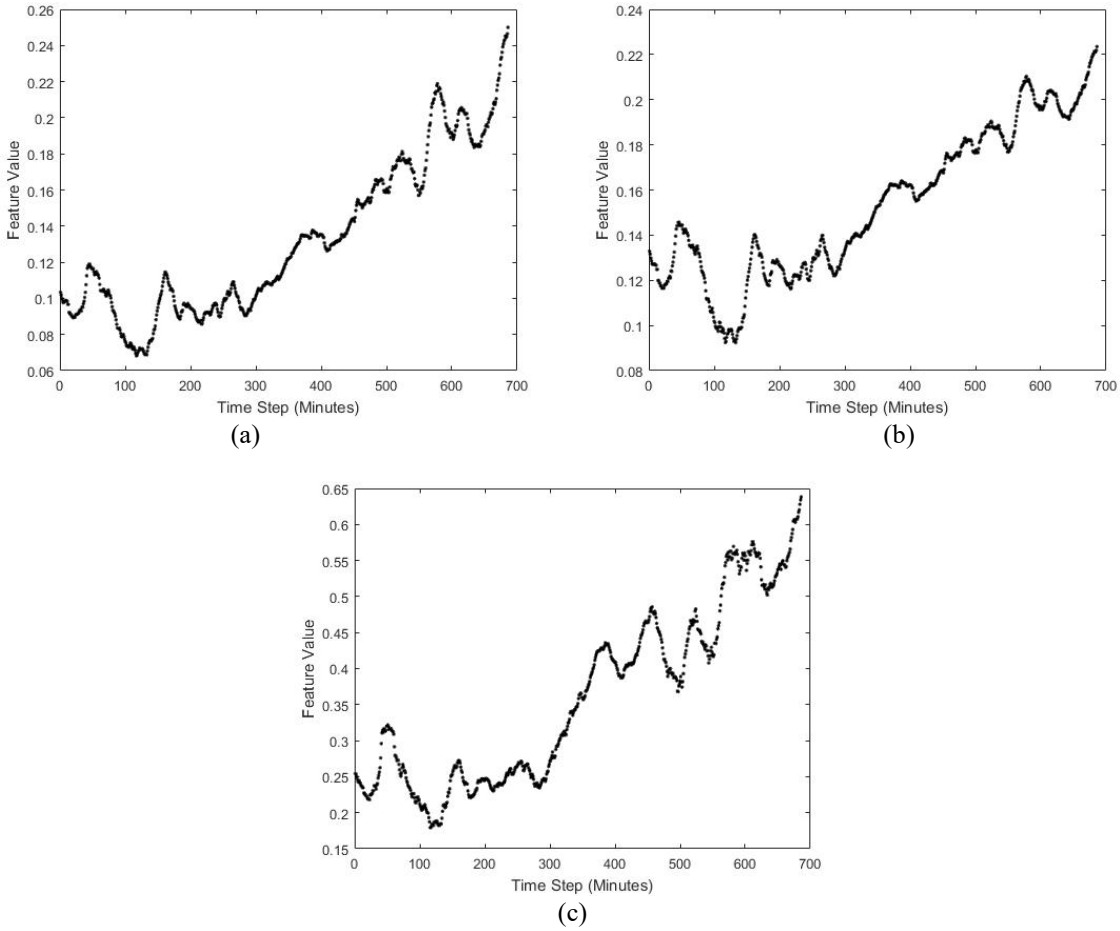

Figure 10. Smoothed feature of (a) RMS, (b) entropy estimation and (c) histogram lower bound.

In Figure 10(a) to 10(c), the features increase drastically after the time step of 300 minutes. It is an indication that the damage to the motor shaft is growing and getting worse. This condition matches the increasing of the FI values of the selected features.

RUL Prediction Using the RMS Feature

The failure threshold is set at the maximum value of the RMS feature. The RUL prediction is initiated at t_P = 343 minutes or 50% of the motor shaft life cycle. At this point, the feature value increases continuously as an indication that the failure is growth. The first data until the prediction start time is treated as the training data, while the rest is set as the testing data. The prediction start time is updated every 10% additional data. So, the prediction was done at t_P = 343, 412, 481, 550 and 619 minutes.

Figure 11 shows that the RUL prediction using a smoothed RMS feature gives satisfactory performance except for prediction at t_P = 412 minutes as in Figure 11(b). The RUL predictions that are shown by the dash-dot line are close to the actual values (the cross mark). Most of the real data are fall within the 95% prediction interval covered by the shaded area. Table 2 presents the complete prediction performance of the motor shaft RUL estimation using smoothed RMS. The table shows that the RUL error is getting smaller when the training data increases. Moreover, the prediction gives the same result as the actual RUL at t_P = 550 minutes.

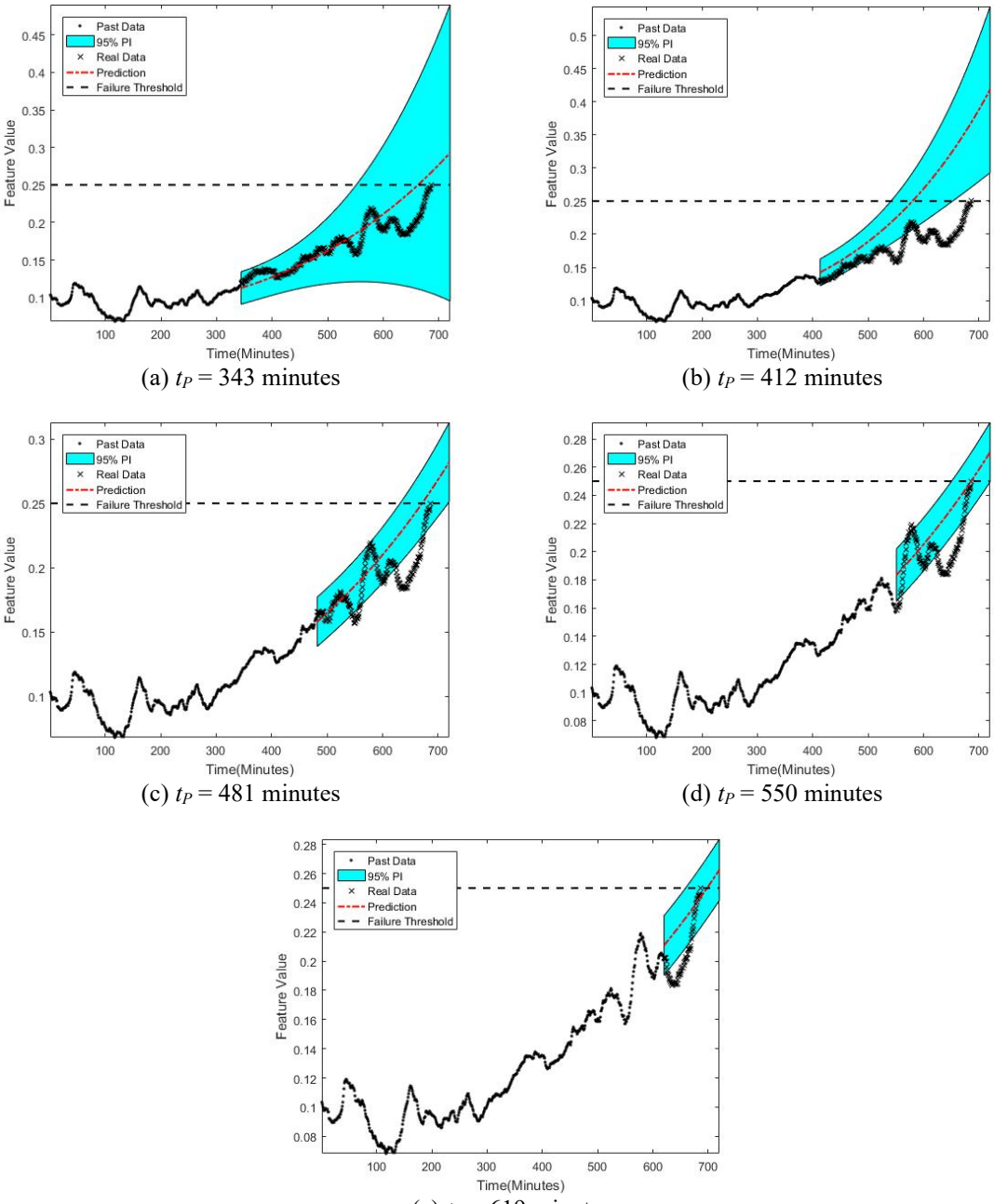

(a) t_P = 343 minutes

(b) t_P = 412 minutes

(c) t_P = 481 minutes

(d) t_P = 550 minutes

(e) t_P = 619 minutes

Figure 11. Motor shaft RUL prediction using smoothed RMS feature.

Table 2. RUL prediction performance using RMS feature.

t_P	Actual RUL	Predicted RUL	RUL error	RMSE
343	343	320	23	0.1341
412	274	168	106	0.9415
481	205	191	14	0.2079
550	136	136	0	0.1712
619	67	79	12	0.1777

RUL Prediction Using Entropy Estimation Feature

The results of motor shaft RUL prediction using the smoothed entropy estimation feature are presented in Figure 12. The prediction result at the earliest start time in Figure 12(a) is far away from the actual RUL even though the actual RUL still in the 95% PI. The RUL prediction is less than the actual RUL. The worse result is found at t_P = 412 minutes as in Figure 12(b). The actual RUL is beyond the 95% PI. However, the updating of the training data in Figure 12(c), 12(d), and 12(e) yield better RUL prediction. The RUL errors become smaller. The complete results are presented in Table 3.

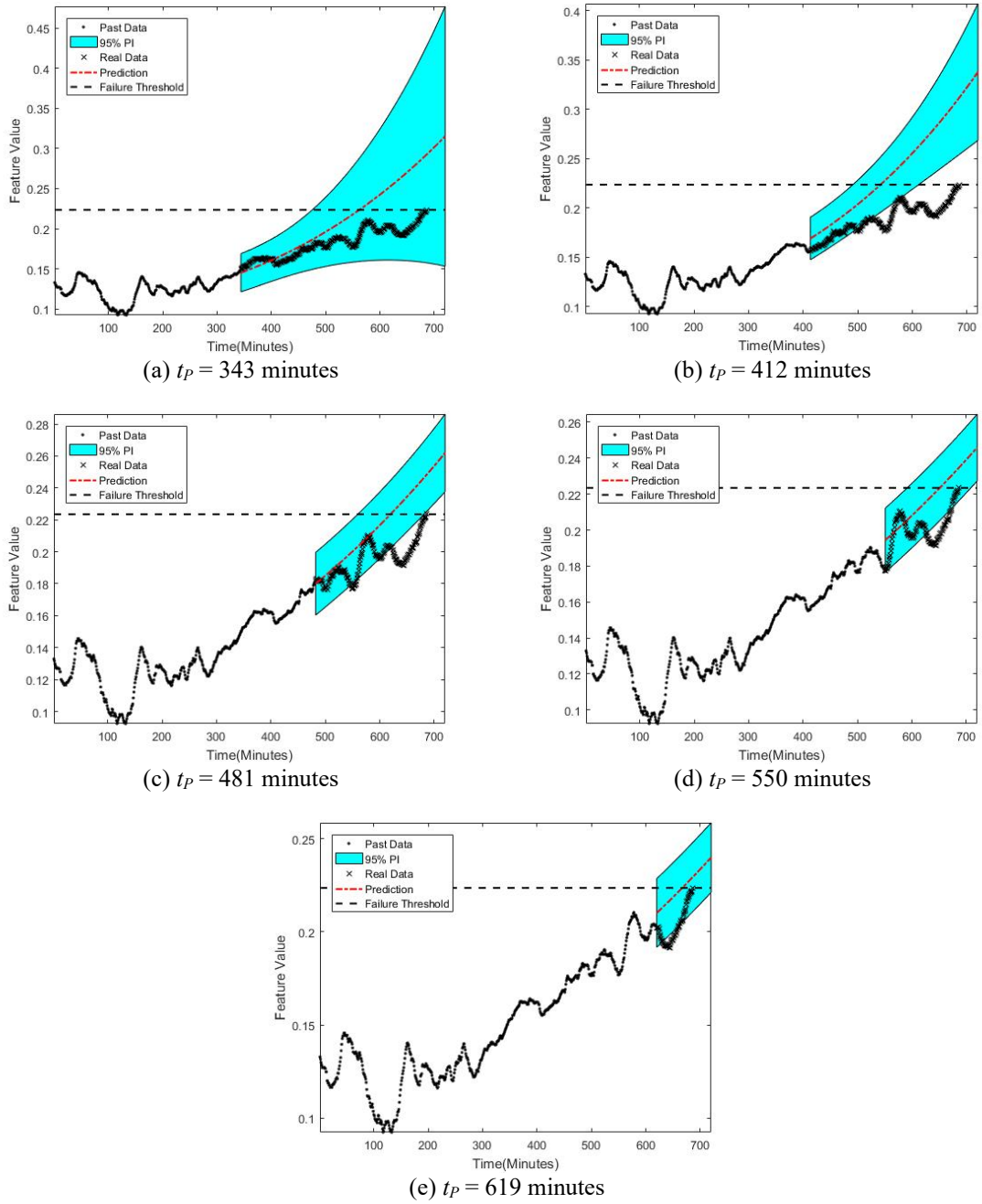

(a) t_P = 343 minutes (b) t_P = 412 minutes

(c) t_P = 481 minutes (d) t_P = 550 minutes

(e) t_P = 619 minutes

Figure 12. RUL prediction using smoothed entropy estimation feature.

Table 3. RUL prediction performance using smoothed entropy estimation feature

t_P	Actual RUL	Predicted RUL	RUL error	RMSE
343	343	219	124	0.4725
412	274	130	144	0.7852
481	205	139	66	0.2475
550	136	102	34	0.1535
619	67	48	19	0.1356

RUL Prediction Using the Histogram Lower Bound Feature

The results of the motor shaft RUL prediction using the smoothed histogram lower bound feature are presented in Figure 13. The prediction results at t_P = 343, 412, and 488 minutes are far away from the actual values as shown in Figure 13(a) to 13(c). The actual RUL values are beyond the 95% PI. The prediction is getting better after t_P = 550 minutes; as in Figure 13(d). The RUL error is small, and the actual RUL is within the 95% PI. The complete performance of motor shaft RUL prediction using smoothed histogram lower bound feature is presented in Table 4. It shows that only prediction at t_P = 550 and 619 minutes fall within acceptable error.

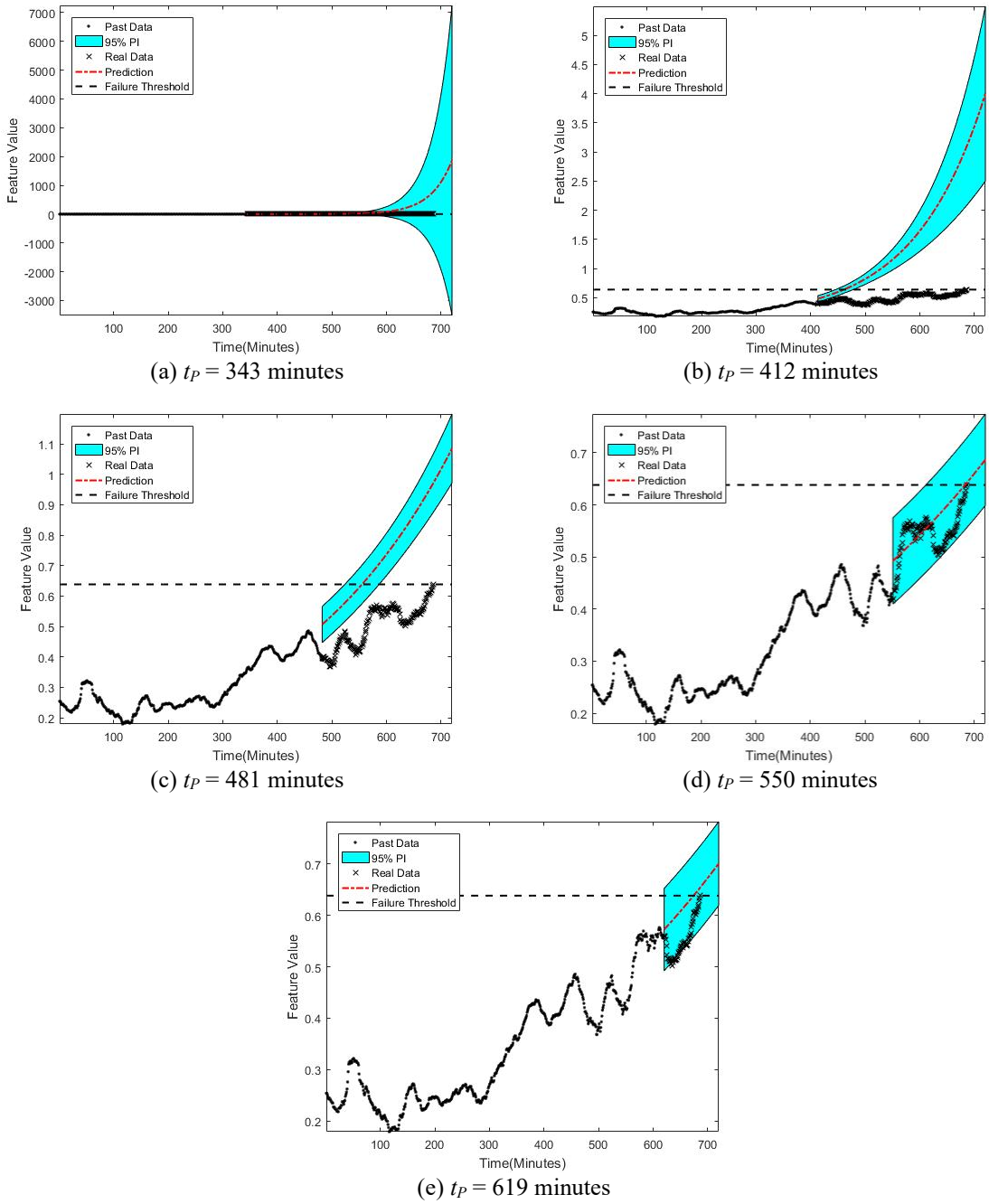

(a) t_P = 343 minutes

(b) t_P = 412 minutes

(c) t_P = 481 minutes

(d) t_P = 550 minutes

(e) t_P = 619 minutes

Figure 13. RUL prediction using the smoothed histogram lower bound feature.

Table 4. RUL prediction performance using the smoothed histogram lower bound feature.

t_P	Actual RUL	Predicted RUL	RUL Error	RMSE
343	343	47	296	1660
412	274	47	227	15.4369
481	205	75	130	3.021
550	136	135	3	0.2503
619	67	55	12	0.4973

RUL Prediction Performance Comparison

The performance of the proposed prognostic method using different features was evaluated using the $\alpha - \lambda$ performance. The α value was set to 0.2, and the λ was 0.5. The accuracy is presented in Figure 14. It can be seen in Figure 14 that the RMS feature performs well for the motor shaft RUL prediction. The prediction at almost each time step falls in the accuracy cone area except for $t_P = 412$ minutes. However, the entropy estimation and histogram lower bound features do not perform well at the early stages of the prediction, with the results being far from the accuracy cone area. Nevertheless, after the prediction time passed halfway to failure from the first prediction was made ($\lambda = 0.5$), the accuracy of the prediction using all of the features was close to the actual RUL.

The selected features, especially RMS can be used as a prognostic indicator to estimate the RUL of the motor shaft. The estimation can be done at an early stage (50% of the motor shaft life) when the initial fault is detected. The prediction accuracy gets better as the life of the motor shaft approaches the end. This result gives enough time for maintenance management to arrange for a maintenance strategy to avoid a catastrophic failure of the induction motor, possibly leading to a loss of production.

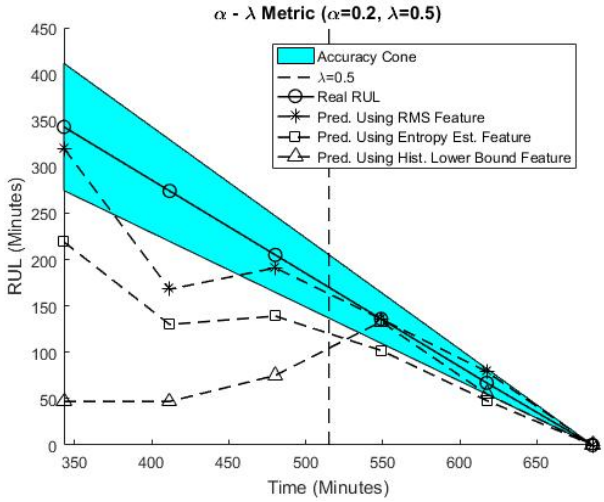

Figure 14. Accuracy of the proposed method using selected features.

CONCLUSION

This paper presents a prognostic method based on the Feature Importance (FI) and LS-SVM regression model to predict the RUL of an induction motor shaft experiencing a keyway failure. The FI is constructed from the superposition of the feature monotonicity and trendability characteristic. The FI of the features is evaluated for a different number of training data. Features having high FI values are selected as the prognostic indicator. They are RMS, entropy estimation, and histogram lower bound. The prediction start time is determined when the value of the feature increases drastically. It starts at $t_P = 343$ minutes or 50% of the motor life. The results show that the RMS feature provided the best prediction results. The RUL prediction using the RMS feature falls in the accuracy zone, except for $t_P = 412$ minutes. However, the other two features do not perform well in predicting the motor shaft RUL in the early stages of the prediction. However, with the increase in the training data, the result becomes more accurate. At 20% before the end of the motor shaft life, the RUL prediction using all of the prognostic indicators are close to the actual RUL. It means that the prognostics using the proposed method provide enough time for maintenance management to take action for avoiding sudden failures of the motor shaft.

The proposed method is applied to the induction motor shaft fault. The degradation profile of the fault follows the exponential form. In practice, different degradation profiles may be encountered. Further examination should be carried out. Moreover, the induction motor can experience multiple failures such as bearing, winding, or rotor failure simultaneously. It can be a challenge for the method in the future to evaluate its performance as a tool for RUL prediction.

REFERENCES

[1] Ergin S, Uzuntas A, Gulmezoglu MB. Detection of stator, bearing and rotor faults in induction motors. Procedia Engineering 2012; 30(2011): 1103–1109.

[2] Raut SP, Raut LP. A review of various methodologies used for shaft failure analysis. International Journal of Engineering Research and General Science 2014; 2(2): 159–171.

[3] Bonnett AH. Root cause ac motor failure analysis with a focus on shaft failures. IEEE Transactions on Industry Applications 2000; 36(5): 1435–1448.

[4] Raut LP, Raut SP. Failure analysis and redesign of shaft of overhead crane. International Journal of Engineering Research and Applications 2014; 4(6): 130–135.

[5] Basu S, Chaure G. Experimental analysis of failure of drive shafts. International Journal of Innovations in Engineering and Technology 2016; 6(3): 254–262.

[6] Hariom VK, Chandrababu D. A review of fundamental shaft failure analysis. International Research Journal of Engineering and Technology 2016: 389–395.

[7] Jardine AKS, Lin D, Banjevic D. A review on machinery diagnostics and prognostics implementing condition-based maintenance. Mechanical Systems and Signal Processing 2006; 20(7): 1483–1510.

[8] Mehala N, Dahiya R. Motor current signature analysis and its applications in induction. International Journal of Systems Applications, Engineering & Development 2007; 2(1): 29–35.

[9] Gupta K, Kaur A. A review on fault diagnosis of induction motor using artificial neural networks. International Journal of Science and Research 2012; 3(7): 680–684.

[10] Bhowmik PS, Pradhan S, Prakash M. Fault diagnostics and monitoring methods of induction motor: A review. International Journal of Applied Control, Electrical and Electronics Engineering 2013; 1(1): 1–18.

[11] Alsaedi MA. Fault diagnosis of three-phase induction motor: A review. Optics 2015; 4(1): 1-8.

[12] Ameid T, Menacer A, Talhaoui H, Harzelli I. Rotor resistance estimation using extended Kalman filter and spectral analysis for rotor bar fault diagnosis of sensorless vector control induction motor. Measurement 2017; 111: 243–259.

[13] Gangsar P, Tiwari R. Signal based condition monitoring techniques for fault detection and diagnosis of induction motors: a state-of-the-art review. Mechanical Systems and Signal Processing 2020; 144: 106908.

[14] Fu P, Wang J, Zhang X, et al. Dynamic routing-based multimodal neural network for multi-sensory fault diagnosis of induction motor. Journal of Manufacturing Systems 2020; 55: 264–272.

[15] Kraleti RS, Zawodniok M, Jagannathan S. Model based diagnostics and prognostics of three-phase induction motor for vapor compressor applications. In: 2012 IEEE Conference on Prognostics and Health Management, Denver, USA, pp. 1-7; 2012.

[16] Arora TG, Aware M V, Tutakne DR. Life estimation of induction motor insulation under non-sinusoidal voltage and current waveforms using fuzzy logic. International Journal of Electrical and Computer Engineering 2014; 7(12): 1759–1766.

[17] Gaied KS. Wavelet-based prognosis for fault-tolerant control of induction motor with stator and speed sensor faults. Transactions of the Institute of Measurement and Control 2014; 37(1): 100–113.

[18] Babel AS, Strangas EG. Condition-based monitoring and prognostic health management of electric machine stator winding insulation. In: 2014 International Conference on Electrical Machines, Berlin, Germany, pp. 1855–1861; 2014.

[19] Barbieri F, Hines JW, Sharp M, Venturini M. Sensor-based degradation prediction and prognostics for remaining useful life estimation: Validation on experimental data of electric motors. International Journal of Prognostics and Health Management 2015; 6: 1–20.

[20] Singleton RK, Strangas EG, Aviyente S. Extended Kalman filtering for remaining-useful-life estimation of bearings. IEEE Transactions on Industrial Electronics 2015; 62(3): 1781–1790.

[21] Nguyen V, Seshadrinath J, Wang D, Nadarajan S, Vaiyapuri V. Model-based diagnosis and rul estimation of induction machines under interturn fault. IEEE Transactions on Industry Applications 2017; 53(3): 2690–2701.

[22] Ahmad W, Ali Khan S, Kim JM. A hybrid prognostics technique for rolling element bearings using adaptive predictive models. IEEE Transactions on Industrial Electronics 2017; 65(2): 1577–1584.

[23] Jain AK, Lad BK. Prognosticating RULs while exploiting the future characteristics of operating profiles. Reliability Engineering and System Safety 2020; 202: 107031.

[24] Yang F, Habibullah MS, Shen Y. Remaining useful life prediction of induction motors using nonlinear degradation of health index. Mechanical Systems and Signal Processing 2021; 148: 107183.

[25] Wahab AMA, Yusof Z, Rasid ZA, Abu A, Rudin NFMN. Dynamic instability of high-speed rotating shaft with torsional effect. International Journal of Automotive and Mechanical Engineering 2018; 15(4): 6034–6051.

[26] Sachs N. Failure analysis of machine shafts. Efficient Plant Magazine. 16 July 2012.

[27] Heidary H, Oskouei AR, Hajikhani M, Moosaloo B, Najafabadi MA. Acoustic emission signal analysis by wavelet method to investigate damage mechanisms during drilling of composite materials. In: ASME 2010 10th Biennial Conference on Engineering Systems Design and Analysis, Istanbul, Turkey, pp. 409-416; 2010.

[28] Suykens JAK, Vandewalle J. Least squares support vector machine classifiers. Neural Processing Letters 1999; 9(3): 293–300.

[29] Gebraeel N. Sensory-updated residual life distributions for components with exponential degradation patterns. IEEE Transactions on Automation Science and Engineering 2006; 3(4): 382–393.

[30] Eker OF, Camci F, Guclu A, Yilboga H, Sevkli M, Baskan S. A simple state-based prognostic model for railway turnout systems. IEEE Transactions on Industrial Electronics 2011; 58(5): 1718–1726.

[31] Li N, Lei Y, Lin J, Ding SX. An improved exponential model for predicting remaining useful life of rolling element bearings. IEEE Transactions on Industrial Electronics 2015; 62(12): 7762–7773.

[32] He W, Williard N, Osterman M, Pecht M. Prognostics of lithium-ion batteries based on dempster-shafer theory and the Bayesian Monte Carlo method. Journal of Power Sources 2011; 196(23): 10314–10321.

[33] Hu J, Tse PW. A relevance vector machine-based approach with application to oil sand pump prognostics. Sensors 2013; 13(9): 12663–12686.

[34] Saxena A, Celaya J, Saha B, Saha S, Goebe K. On applying the prognostic performance metrics. In: Annual Conference of the Prognostics and Health Management, San Diego, California, pp. 1-16; 2009.